ResearchGate

See discussions, stats, and author profiles for this publication at: https://www.researchgate.net/publication/235421331

Biotransformation Pathways of Biocides and Pharmaceuticals in Freshwater Crustaceans Based on Structure Elucidation of Metabolites Using High Resolution Mass Spectrometry

ARTICLE *in* CHEMICAL RESEARCH IN TOXICOLOGY · FEBRUARY 2013

Impact Factor: 3.53 · DOI: 10.1021/tx300457f · Source: PubMed

READS

82

3 AUTHORS:

Junho Jeon

Changwon National University

16 PUBLICATIONS **246** CITATIONS

SEE PROFILE

Denise Kurth

Helmholtz-Zentrum für Umweltforschung

3 PUBLICATIONS **22** CITATIONS

SEE PROFILE

Juliane Hollender

Eawag: Das Wasserforschungs-Institut des ET…

184 PUBLICATIONS **3,980** CITATIONS

SEE PROFILE

Available from: Junho Jeon
Retrieved on: 29 January 2016

Chemical Research in Toxicology

Article

pubs.acs.org/crt

Biotransformation Pathways of Biocides and Pharmaceuticals in Freshwater Crustaceans Based on Structure Elucidation of Metabolites Using High Resolution Mass Spectrometry

Junho Jeon,[†] Denise Kurth,[†,‡] and Juliane Hollender*[,†,‡]

[†]Eawag, Swiss Federal Institute of Aquatic Science and Technology, 8600 Dübendorf, Switzerland

[‡]Institute of Biogeochemistry and Pollutant Dynamics, ETH Zürich, CH-8092, Zürich, Switzerland

Supporting Information

ABSTRACT: So far, there is limited information on biotransformation mechanisms and products of polar contaminants in freshwater crustaceans. In the present study, metabolites of biocides and pharmaceuticals formed in *Gammarus pulex* and *Daphnia magna* were identified using liquid chromatography−high resolution mass spectrometry. Different confidence levels were assigned to the identification of metabolites without reference standards using a framework based on the background evidence used for structure elucidation. Twenty-five metabolites were tentatively identified for irgarol, terbutryn, tramadol, and venlafaxine in *G. pulex* (21 via oxidation and 4 via conjugation reactions) and 11 metabolites in *D. magna* (7 via oxidation and 4 via conjugation reactions), while no evidence of metabolites for clarithromycin and valsartan was found. Of the 360 metabolites predicted for the four parent compounds using pathway prediction systems and expert knowledge, 23 products were true positives, while 2 identified metabolites were unexpected products. Observed oxidative reactions included N- and O-demethylation, hydroxylation, and N-oxidation. Glutathione conjugation of selected biocides followed by subsequent reactions forming cysteine conjugates was described for the first time in freshwater invertebrates.

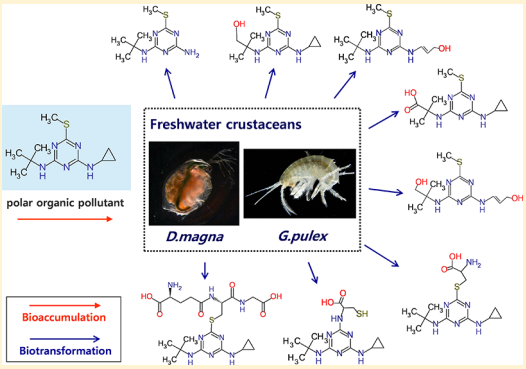

INTRODUCTION

Bioaccumulation is one of the end points in risk assessment of chemicals[1,2] and is often modified by biotransformation, which is a key factor regulating body burden[3−6] and thus the toxicity of organic pollutants.[7,8] Information on bioaccumulation and biotransformation of organic compounds in aquatic organisms other than fish is rather limited.[9] In a few studies, it was shown that biotransformation in freshwater arthropods greatly modified internal concentrations of organic chemicals[3−6,10] and that metabolites were identified for organic pollutants such as poly aromatic hydrocarbons[3,4] and pesticides[5,10] in *Daphnia*.

Although polar compounds (e.g., biocides and pharmaceuticals) have a lower potential to bioaccumulate than nonpolar compounds, they are usually present in surface water at much higher bioavailable concentrations[11,12] and therefore pose a potential risk to aquatic organisms. Due to mandatory registration by governments before usage, some data on biotransformation are available for organic pollutants in target organisms but not for nontarget organisms such as freshwater crustaceans. For example, the biotransformation pathway and metabolites of tramadol, a painkiller, have been intensively studied for target organisms, including humans,[13−15] but no information for ecologically relevant species is available so far. Some previous studies reported on transformation products of irgarol, a biocide, formed by photochemical reaction[16] and their occurrence in the environment;[17] but none of the studies explored metabolites in nontarget organisms.

Enzymatic reactions involved in the metabolism of xenobiotic compounds include oxidations (e.g., hydroxylation, N-, S-oxidation, or dealkylation), reductions (e.g., dehalogenation and hydrolysis of amides and carboxyl esters), and conjugation reactions where functional groups in a reactant are conjugated with endogenous molecules such as carbohydrates, sulfate, glutathione, and amino acids. The metabolic enzymes are diverse, ranging from mixed-function oxidases such as P450 up to esterases, hydrolases, reductases, and transferases. Katagi et al.[9] reported that many enzymatic activities observed in humans and fish have also been described in aquatic invertebrates, although species differences exist.

Metabolites are usually more hydrophilic and less toxic than their parent compounds, resulting in detoxification, but sometimes comparable or even higher toxicity was reported.[18] The desulfuration of organothiophosphate insecticides to oxon-analogues, which are potent acetylcholinesterase inhibitors, is a prominent example of bioactivation. In other examples, the hydrolysis of 2,4-dichlorophenoxyacetic acid to 2,4-dichlorophenol[19] or methylation of triclosan[20] leads to more hydro-

Received: November 14, 2012
Published: February 8, 2013

 © 2013 American Chemical Society

phobic metabolites, which show higher bioaccumulation potential and correspondingly higher baseline toxicity.

Despite their significance in risk assessment, metabolite identification has been limited due to difficulty in the acquisition of either commercially available reference standards or a sufficient amount and purity of metabolites for NMR analysis. Recently, a number of studies have successfully shown the feasibility of high resolution mass spectrometry coupled with liquid chromatography (LC-HRMS) for the tentative identification of metabolites without reference standards.[21−25] However, there is a need to gather additional evidence (e.g., prediction of metabolites using pathway prediction systems, MS/MS fragmentation, physicochemical properties) and sensible guidelines to indicate the reliability of the identification in cases where confirmation with a reference standard or orthogonal analytical methods is not possible.

The aim of this study was to identify metabolites of polar contaminants formed in nontarget freshwater invertebrates using LC-HRMS and subsequently propose biotransformation pathways. As target compounds, two biocides (irgarol and terbutryn) and four pharmaceuticals (tramadol, venlafaxine, valsartan, and clarithromycin) were selected by considering their frequent occurrence in freshwater,[26,27] different physical properties (neutral compounds, cations, anions; log D_{ow} 0.8−2.9) but also common moieties (triazine, dimethylamino-methoxyphenyl) for comparison purposes. To account for species differences in xenobiotic metabolism, two model organisms, *Gammarus pulex* and *Daphnia magna*, were selected. Both are focal organisms for the functioning of aquatic food webs and are already used in risk assessment studies.[28−30] The exposure concentration (100 μg/L) was far below the known acute effect concentrations in the mg/L range to avoid influence on biotransformation but approximately 1000 times higher than freshwater concentrations to enable the detection of metabolites. To overcome the lack of reference standards for metabolites, we developed a framework to classify different confidence levels for metabolite identification. On the basis of these results, biotransformation pathways of the targets in freshwater crustaceans are proposed.

MATERIALS AND METHODS

Chemicals and Solutions. Detailed information on physicochemical properties of the selected compounds, chemical standards, reagents, and solutions used in instrumental analysis and exposure tests are provided in the Supporting Information (SI 1 and Table S1−2).

Test Organisms. *Gammarus pulex* were collected from a small creek in the Itziker Ried a few kilometers southeast of Zurich, Switzerland (Coordinates: E 702150, N 2360850) and acclimatized in an aquarium with aerated artificial pond water (APW) for 3−5 days. During acclimatization and the experiment, *G. pulex* were fed with horse chestnut leaves inoculated with *Cladosporium herbarum*. Detailed information on the preparation of APW and the inoculation of leaves are found elsewhere.[31] All experiments with *G. pulex* were carried out at 13 ± 2 °C and 12 h/12 h light/dark conditions.

Daphnia magna (STRAUS 1820 clone 5) were obtained from the Institute for Environmental Research at the RWTH Aachen University. *D. magna* were cultured in artificial freshwater (M4 medium) at a temperature of 20 ± 2 °C and 16 h/8 h light/dark conditions according to the Organisation for Economic Co-operation and Development guidelines.[32] Adults were kept in glass beakers each containing 20 *D. magna* and approximately 1.5 L of M4 medium. To provide the optimal conditions to adults, neonates were separated from adults at least three times a week and discarded if not needed. The M4 medium was renewed once a week. The green algae *Scenedesmus obliquus* was used as food source, and the *D. magna* were fed with 0.05 mg particulate organic carbon(POC)/daphnia/d for the first week and with 0.1 mg POC/daphnia/d for the 2−4 week old *D. magna*. For exposure experiments, neonates ≤24 h were separated from the third and fourth week of the main culture. These were raised for 5 days under the same temperature−light condition as the main culture. Each beaker contained 40 neonates, which were fed with 0.025 mg POC/daphnia/d. Prior to the experiments, *D. magna* were transferred into clean M4 medium for 1−3 h. For subsequent *in vitro* experiments, *D. magna* were sieved, washed with water, frozen in liquid nitrogen, and stored at −80 °C until further analysis. In the case of *in vivo* exposure, *D. magna* were directly transferred into the exposure medium.

***In Vivo* Experiments.** The specific conditions of *in vivo* experiments for each organism is described below in parentheses as follows (condition for *G. pulex*: for *D. magna*). The exposure solutions were prepared (in APW: in M4 medium) at nominal concentration, 100 μg/L for each target compound. Glass beakers (600 mL/50 mL) in replicate (duplicate/triplicate) per compound were filled with exposure solution (500 mL/30 mL). Inoculated horse chestnut leaves were added only to *G. pulex* experiments as food source. Then, organisms (5−6: about 30 individuals) were introduced into the beakers and incubated in a temperature-control chamber (13 °C/ 20 °C). After 24 h of exposure, the organisms were sieved, blotted dry on tissue, collected in a 2 mL microcentrifuge tube, weighed, and shock frozen in liquid nitrogen. The exposure solutions were also sampled at the beginning and end of exposure, filtered with a 0.2 μm cellulose filter, and kept at −80 °C until further preparation. For the chemical extraction, a FastPrep-24 bead beater (MP Biomedicals, Switzerland) was used. Three hundred milligrams of 1 mm zirconia/silica beads (BioSpec Products, Inc., USA), 200 mL of a stable isotope-labeled internal standard at 100 ng/mL of each target compound in methanol, and 800 mL of methanol were added to each microcentrifuge tube where exposed organisms were collected. After capping the tubes, the samples were placed in the FastPrep and homogenized twice for 15 s at 6 m/s and cooled on ice in between. The extracts were filtered with a 0.2 μm cellulose filter (BGB Analytic AG, Switzerland) and kept at −80 °C until LC-HRMS analysis. Two different controls, i.e., without target chemicals (chemical-negative) and without test organisms (organism-negative), were treated similarly. To verify metabolites formed by the food source, an additional control (chemical-food positive, but *G. pulex* negative) was also performed.

***In Vitro* Experiments.** For *in vitro* tests, nonexposed *G. pulex* and *D. magna* were homogenized in phosphate (PP) buffer solution (0.05 M, pH 7.2) as described elsewhere[33,34] and modified as follows. Approximately, 6 *G. pulex* or 200 *D. magna*, which were stored at −80 °C, were homogenized in 1 mL of PP buffer with an ultrasonic homogenizer Labsonic M (Sartorius Stedim Biotech, Switzerland) (3 × 30 s with an amplitude of 100% and a cycle of 1.0 with 15−30 s break in between). The samples were cooled on ice during ultrasonication. The homogenates obtained were centrifuged at 10000*g* at 4 °C for 10 min. Supernatants were collected and used as enzyme extracts. For *in vitro* exposure tests, 100 μL of the extracts were spiked with 100 μL of the individual target compound in PP buffer (300 μg/L) and 100 μL of 1.0 mM NADPH in PP buffer and incubated for 2 h at 13 °C (*G. pulex*) and 20 °C (*D. magna*). The reaction was terminated by adding 1 mL of methanol. The samples were filtered (0.2 μm) and kept at −80 °C until LC-HRMS analysis. To verify the *in vitro* experimental method, rat liver S9 homogenate (37.5 mg protein/mL, MP Biomedicals, Switzerland) was similarly processed.

Biotransformation Products Prediction. Two different *in silico* predictions were used to identify possible metabolite structures: University of Minnesota Pathway Prediction System (UM-PPS) and Meteor Environmental Pathway Prediction System (Lhasa Limited, UK). The UM-PPS predicts microbial metabolic reactions based on biotransformation rules set in the University of Minnesota Biocatalysis/Biodegradation Database and literature.[35] The meteor was built from mammalian biotransformation reactions of common functional groups/drugs and allows selection of the most probable

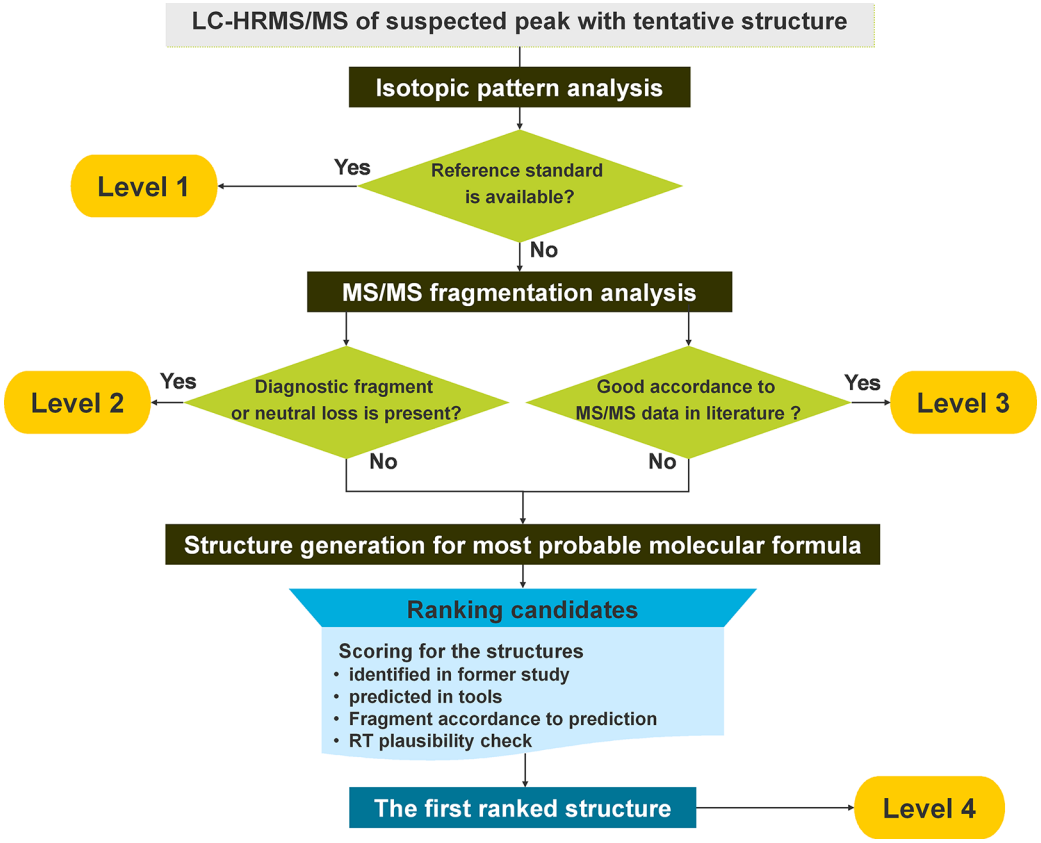

Figure 1. Schematic procedure for structure elucidation of metabolites and classified confidence level for identification.

transformation products as well as providing information on possible literature references.[36] The prediction results from both programs include the exact masses and structures of metabolites generated from four subsequent reactions in the metabolic pathway. In addition to the *in silico* predictions, a "manual" prediction considering common metabolic reactions as described elsewhere[37] was performed. The prediction results were used to build a mass list of suspected metabolites, which was inserted into the instrumental method file for data-dependent MS/MS acquisition as described below.

LC–High-Resolution Mass Spectrometry. Extracts from *in vivo* and *in vitro* experiments and exposure solutions were analyzed with liquid chromatography–electrospray–high resolution tandem mass spectrometry (LC-ESI-HRMS/MS). Automated online solid phase extraction was applied to avoid contamination of the mass analyzer by matrix components. A mixed bed multilayer cartridge (10 mg Oasis HLB (Waters, USA) above a 10 mg mixture of ENV+ (International Sorbent Technology, UK), Strata X-AW, and X-CW (Phenomenex, UK)) was used to enrich a broad range of parent compounds as well as small and ionic metabolites. The instrumental hardware for online enrichment was described in Singer et al.[38] One hundred microliters of sample extracts were injected into 20 mL headspace glass vials, which were then filled with deionized water. To confirm the presence of low intensity peaks, some samples were reanalyzed with an increased extraction volume (500 μL). The mobile phase (HPLC-grade water and methanol with 0.1% (vol.) formic acid) was pumped into a Waters Atlantis T3 3 mm column (3.0 × 150 mm) at 300 μL/min using a binary pump (Rheos 2000, Flux Instruments, Switzerland). Before sample injection, the loop was rinsed with HPLC-grade acetonitrile at a flow rate of 2000 μL/min using an isocratic pump (Rheos 2000, Flux Instruments, Switzerland). The samples were then injected together with the loading solution as described in Table S4 (Supporting Information). Detection of analytes was performed with a Linear Trap Quadrupole Orbitrap mass spectrometer (Thermo Scientific, Switzerland) with an ESI interface in positive and negative mode, with the following parameters: sheath gas flow (40 L/min), auxiliary gas flow (20 L/min), and capillary temperature (300 °C). Source voltage, tube lens, and capillary voltage were set to 4.5 kV, 60 V, and 35 V in positive mode and −4 kV, −110 V, and −35 V in negative mode, respectively. A mass range of 150–2000 m/z was analyzed in full scan with a maximal ion count of 1,000,000. External mass calibration was used to ensure a mass accuracy of <5 ppm over the MS mass range. The Orbitrap operation method was designed to perform data-dependent MS/MS fragmentation (DDF) for the five most intense ions among the mass list of predicted metabolites at each scan event. During the MS/MS acquisition, a dynamic exclusion function was applied to prevent an ion from triggering a subsequent DDF for 10 s once it had already triggered a DDF scan. If no mass from the list of predicted metabolites was found, the most intense ions were fragmented. The optimum collision energy for DDF with higher energy collision dissociation (HCD) was estimated using an empirical linear equation, which is a function of exact mass. High-resolution mass spectra were recorded with a resolution of 60,000, while DDF scans were acquired at a resolution of 7,500.

Data were analyzed with Xcalibur (Thermo Scientific, Switzerland) in the Quan Browser for quantitative analysis with reference standards and in the Qual Browser for identification. Parent compounds in the exposure medium and the organisms were quantified using the stable isotope-labeled internal standards.

Procedure for structure elucidation. For the structure elucidation, a systematic procedure was established to classify confidence in structure identification (Figure 1). Once suspected peaks were identified with tentative structures, isotopic pattern analysis was performed. Then, the structure identification steps assigning different confidence levels were followed. A structure confirmed with the standard was given the highest confidence level, Level 1. If no standard was available, MS/MS fragmentations were analyzed using fragmentation prediction tools and expert knowledge. The fragmentation patterns were evaluated to check if diagnostic fragments which could only be generated from a specific structure or diagnostic neutral losses which are characteristic of molecules with a certain substructure

dx.doi.org/10.1021/tx300457f | *Chem. Res. Toxicol.* 2013, 26, 313–324

Table 1. Overview of Identified Biotransformation Products Formed in Freshwater Crustaceans

parent compound, formula, log D_{ow} at pH 7.9, $[M+H]^+$, t_R (min)[a]	BAF[b] (AVG ± SD, kg/L)	metabolite Name[c]	measured $[M+H]^+$ of metabolites (mass error, ppm)	t_R (min)	log D_{ow} at pH 7.9[a]	molecular formula change	exposure sample[d]	confidence level[e]
irgarol, $C_{11}H_{19}N_5S$, log D_{ow} 2.94, $[M+H]^+$: 254.1434, t_R: 16.1	G: 19.4 ± 3.2	MIR214	214.1118 (−1.40)	14.6	2.21	-C_3H_4	G, D, GS10, DS10, S9	1
		MIR270A	270.1385 (0.74)	14.7	1.94	+O	G, D, GS10, S9	2
		MIR270B		15.8	2.07		G, D, GS10, S9	3 [16]
		MIR284	284.1174 (−0.70)	14.6	−1.81	-H_2+O_2	G	2
		MIR286	286.1331 (−0.35)	14.3	1.08	+O_2	G, GS10, S9	2
	D: 9.7 ± 4.0	MIR327A	327.1606 (2.45)	13.9	−2.43	+$C_2H_3NO_2$	G, D, S9	2
		MIR327B		14.9	−3.8		G, D, S9	2
		MIR513	513.2245 (1.36)	14.4	−10.23	+$C_9H_{13}N_3O_6$	G, S9	2
terbutryn, $C_{10}H_{19}N_5S$, log D_{ow} 2.79, $[M+H]^+$: 242.1434, t_R: 15.7	G: 15.3 ± 1.5	MTE214	214.1119 (−0.93)	14.7	2.21	-C_2H_4	G, D, S9	1
		MTE258A	258.1384 (0.39)	14.5	1.83	+O	G, D	2
		MTE258B		15.6	1.83		G, D, GS10, DS10, S9	2
		MTE272	272.1174 (−0.73)	14.2	−1.91	-H_2+O_2	G, S9	2
	D: 4.7 ± 1.8	MTE315A	315.1602 (1.27)	14.1	−2.53	+$C_2H_3NO_2$	G, D, S9	2
		MTE315B		14.7	−3.90		G, D, S9	2
		MTE501	501.2236 (−0.4)	14.3	−10.34	+$C_9H_{13}N_3O6$	G, S9	2
tramadol, $C_{16}H_{25}NO_2$, log D_{ow} 1.33, $[M+H]^+$: 264.1958, t_R: 12.5	G: 1.5 ± 0.5	MTR236	236.1642 (−1.27)	11.8	−0.09	-C_2H_4	G	4
		MTR250	250.1800 (−0.80)	11.3	0.94	-CH_2	G, D, S9	2
		MTR266	266.1750 (−0.38)	11.9	1.16	-CH_2 +O	G	3 [13]
	D: 1.9 ± 0.8	MTR280A	280.1906 (−0.36)	11.1	0.00	+O	G	3[13,14]
		MTR280B		12.7	1.33		G	3[13,15]
venlafaxine, $C_{17}H_{27}NO_2$, log D_{ow} 1.95, $[M+H]^+$: 278.2115, t_R: 13.5	G: 1.0 ± 0.2	MVE250	250.1798 (−1.6)	12.3	0.32	-C_2H_4	G	1
		MVE264A	264.1960 (−0.76)	12.3	1.54	-CH_2	G, GS10, S9	1
		MVE264B		13.6	0.47		G, GS10	1
	D: 1.6 ± 0.2	MVE280	280.1906 (−0.36)	12.0	0.15	-CH_2+O	G	4
		MVE294	294.2060 (−0.34)	12.1	0.30	+O	G	4

[a]Predicted by MarvinSketch, version 5.4.1.1. [b]G: *G. pulex*. D: *D. magna*. BAF for valsartan and clarithromycin are G: 2.2 ± 0.8.; D: 1.6 ± 0.4; and G, 4.5 ± 1.2; D, 3.3 ± 0.8, respectively. [c]Nomenclature: M stands for metabolite, the following two alphabet letters represent the first two letters of the name of the parent compound, the following three figures represent $[M+H]^+$ of the metabolite, and A or B at the end is a differentiator for metabolites having the same exact mass. [d]Type of exposure sample in which the metabolite was identified: G and D from an *in vivo* test with *G. pulex* and *D. magna*, respectively; GS10, DS10, and S9, from an *in vitro* test with *G. pulex*, *D. magna*, and rat liver homogenate, respectively. [e]Level 1, confirmed with reference standard in this study; level 2: if a diagnostic fragment was detected; level 3, if good accordance with fragmentations reported in literature; level 4, the first ranked structure by candidate ranking system.

were present (Level 2) or whether the measured MS/MS spectra were comparable to those reported in literature (Level 3). In case that a structure has been already reported with diagnostic fragments or neutral losses, Level 2 is given. For all unidentified metabolites, structure generation was used as described elsewhere,[39] and resulting structures were ranked by comparing the predicted and measured MS/MS fragmentation. The first ranked candidate was defined as a Level 4 tentatively identified structure. For the structures with Levels 2, 3, and 4, retention time (t_R) plausibility checks were performed based on the t_R prediction established by the correlation between t_R and hydrophobicity. If the predicted t_R for the elucidated structure was within 2 min of the observed t_R, we considered it a plausible structure. Details on the candidate ranking and the t_R prediction are presented in SI 2 (Supporting Information). Metabolites of Levels 2, 3, and 4 are only tentatively identified because confirmation with a reference standard or orthogonal analytical methods was not possible.

Software Tools and Data Analysis. MetWorks 1.3 and SIEVE V.1.2 (Thermo Scientific, Switzerland) were used to extract candidate ions for predicted and unpredicted metabolites from the extracted ion chromatograms, respectively. Detailed information on settings are given in SI 3 (Supporting Information).

The MS/MS fragmentation of suspected structures was predicted using Mass Frontier 6.0 (HighChem, Ltd., Bratislava, Slovakia) and MetFrag (http://msbi.ipb-halle.de/MetFrag/), and then compared with the measured fragments. For metabolites of Level 4, all possible structures were generated using MOLGEN 3.5[40] using substructure restrictions consistent with the analytical data. The chromatographic t_R of all structures was estimated using molecular weight and hydrophobicity (see SI 2, Supporting Information).

dx.doi.org/10.1021/tx300457f | *Chem. Res. Toxicol.* 2013, 26, 313−324

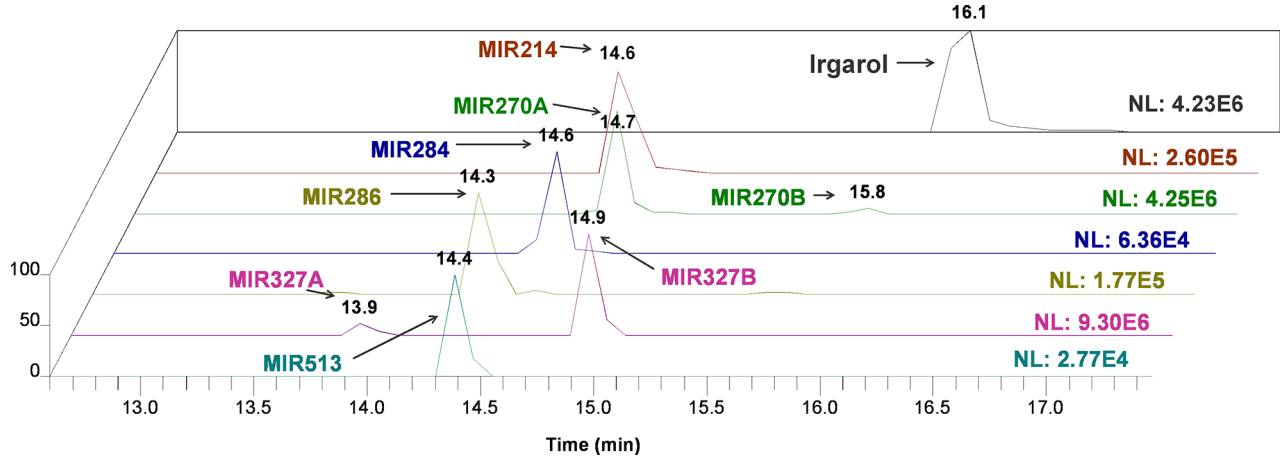

Figure 2. Extracted ion chromatograms of irgarol and its metabolites with retention time and normalized largest peak intensity (NL).

On the basis of the fact proved elsewhere[41,42] that the concentrations has reached equilibrium within 24 h, bioaccumulation factors (BAFs) for parent compounds were calculated using the ratio of the concentration in organism and exposure media measured at t = 24 h.

RESULTS AND DISCUSSION

Bioaccumulation of Parent Compounds. Information on recovery, limit of detection (LOD), and concentration of parent compounds in exposure media and organisms are provided in Table S5 (Supporting Information). After 24 h of exposure, the aqueous concentrations of parents decreased by 5−31% in the presence of and 0−21% in the absence of organisms. Next to dissipative processes such as sorption to glassware, the slightly higher decrease with organisms indicates some partitioning to organisms. The estimated BAF values (Table 1) were greater for the neutral biocides (BAF = 4.7−19.4) than for the charged pharmaceuticals (1.0−4.5) in both organisms and correlated with the log D_{ow} values. Generally, bioaccumulation was greater in *G .pulex* than in *D. magna*, which can be explained by the higher lipid content.[43] The slightly lower BAFs observed for venlafaxine and tramadol may imply that those compounds are more rapidly biotransformed in *G. pulex* than in *D. magna*, although the charge states of those compounds may also explain this observation. The BAFs for *D. magna* are in the same order of magnitude as the values predicted using the model of Geyer et al.[44] (Table S1, Supporting Information).

Overview of Identified Metabolites. Full scan HRMS files of controls and exposure samples were evaluated for the identification of predicted/unpredicted metabolites through suspect/nontarget screening using software tools (MetWorks/SIEVE). Ions detected only in the exposure samples with an intensity above 10^4 and found in all replicates were considered suspected metabolites. No suspected metabolites were found in the controls except N-desmethyltramadol, which exhibited the same extent in the organism-negative control and was therefore excluded from metabolite evaluation. For irgarol, terbutryn, tramadol, and venlafaxine, 25 chromatographically resolved peaks were observed corresponding to 19 unique m/z values. Two isobaric species were observed for six different m/z values (see Table 1). Five metabolites were confirmed with reference standards (Level 1), while 13, 4, and 3 metabolites were tentatively identified with confidence Levels 2, 3 and 4, respectively. In contrast, no evidence of metabolites for clarithromycin and valsartan was found, even though these compounds showed higher BAF values than tramadol and venlafaxine. Clarithromycin has several polar functional groups including three hydroxyl groups so that further functionalization may not be triggered. The relatively higher LOD for valsartan (Table S5, Supporting Information) could be a reason for the lack of observed metabolites. The numbers of predicted metabolites for the four parent compounds are 97, 93, and 360 by UM-PPS, Meteor, and manual prediction, respectively. All metabolites predicted by UM-PPS and Meteor were covered by the manual prediction. Among the 360 predicted metabolites, 23 products of the four compounds were identified through suspect screening of the predicted potential metabolites within the full-scan data, while the two glutathione products of irgarol and terbutryn were recognized later with literature data[45] when researching the formation of cysteine conjugates. Nontarget screening without use of prior knowledge using SIEVE highlighted four relatively intense peaks corresponding to hydroxylation and cysteine conjugation products of irgarol and terbutryn (also identified through suspect screening) but did not find unpredicted metabolites.

All identified metabolites were detected in ESI positive mode, while no peaks in the negative mode could be identified. The metabolites listed in Table 1 were all identified in the extract of *in vivo G. pulex* samples; some were also detected in *D. magna* or in *in vitro* assays. Mass errors between theoretical and measured mass for metabolites were within ±2.5 ppm. Mass changes suggested molecular modifications mainly via dealkylation, oxidation, and glutathione conjugation processes, supported by shorter t_R for almost all metabolites compared to their parent compounds. Only MTR280B (N-oxidation) and MVE264B (N-demethylation) showed a slight t_R increase of 0.1 and 0.2 min, respectively, which was also observed in a previous study,[15] indicating less influence of the N-modifications on the overall polarity of the molecules.

No acute toxicity of formed metabolites were found during the 24 h exposure. The estimated hydrophobicity (i.e., log D_{ow}) of identified metabolites was less than their parent compounds (Table 1), indicating the reduction of baseline toxicity by biotransformation reactions. However, some metabolites seem to have toxic potential. For example, it was reported that cysteine derivatives (e.g., MIR327A or MTE315A) can form reactive intermediates exerting cytotoxicity to kidney cells[46] or acute toxicity toward *Daphnia*.[47] In addition, products with aromatic amine groups (e.g., MIR214 and MTE214), which

dx.doi.org/10.1021/tx300457f | *Chem. Res. Toxicol.* 2013, 26, 313−324

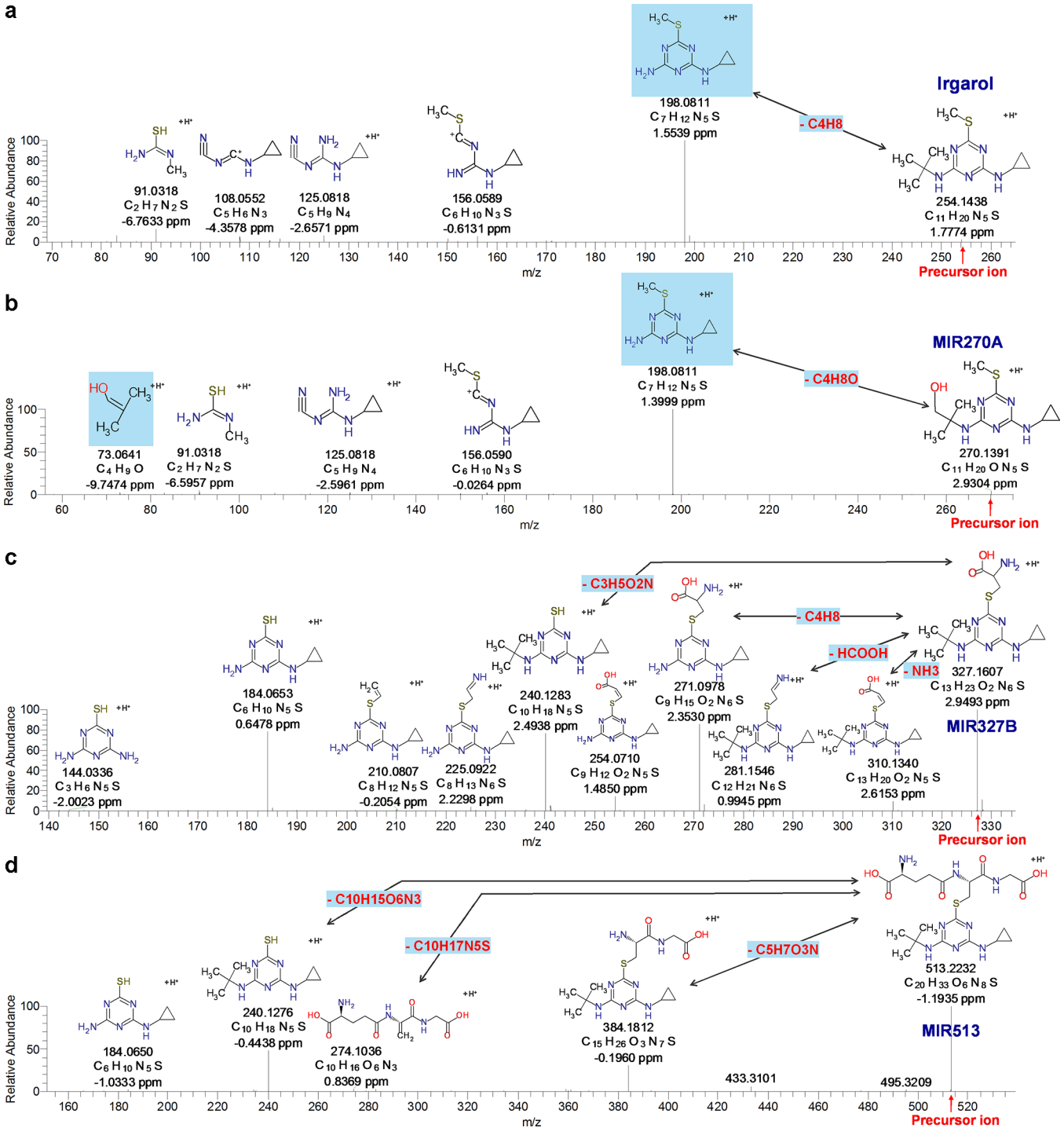

Figure 3. MS/MS spectra for irgarol (a) and the three key metabolites, MIR270A, MIR327B, and MIR513, with proposed fragment structures (b–d). Double-headed arrows indicate the difference in molecular formula between two structures. The shaded structures and molecular formulas represent diagnostic fragments or neutral losses.

would be considered as mutagens,[48] have revealed at least 10 times greater toxicity toward the root elongation of a higher plant than their parents, whereas less toxicity was shown for algae, bacteria, and aquatic crustaceans.[17]

Structure Elucidation. *Irgarol/Terbutryn.* Figure 2 shows extracted ion chromatograms of irgarol and its eight metabolites, while Figure 3 depicts MS/MS fragmentation patterns and proposed structures of irgarol and its three key metabolites in the pathway (Figure 4). MIR270A and MIR327B are the major oxidation and conjugation product, respectively, with relatively high peak intensity. The glutathione conjugate, MIR513, is an intermediate product of the cysteine conjugate, MIR327B, which was observed for the first time in the test organisms. Results for the other metabolites are shown in Figures S1 (irgarol), S2 (terbutryn), S3 (tramadol), and S4 (venlafaxine) (Supporting Information). Descyclopropyl-irgarol (MIR214) was confirmed by a reference standard and has been identified as a major transformation product formed by a

dx.doi.org/10.1021/tx300457f | Chem. Res. Toxicol. 2013, 26, 313–324

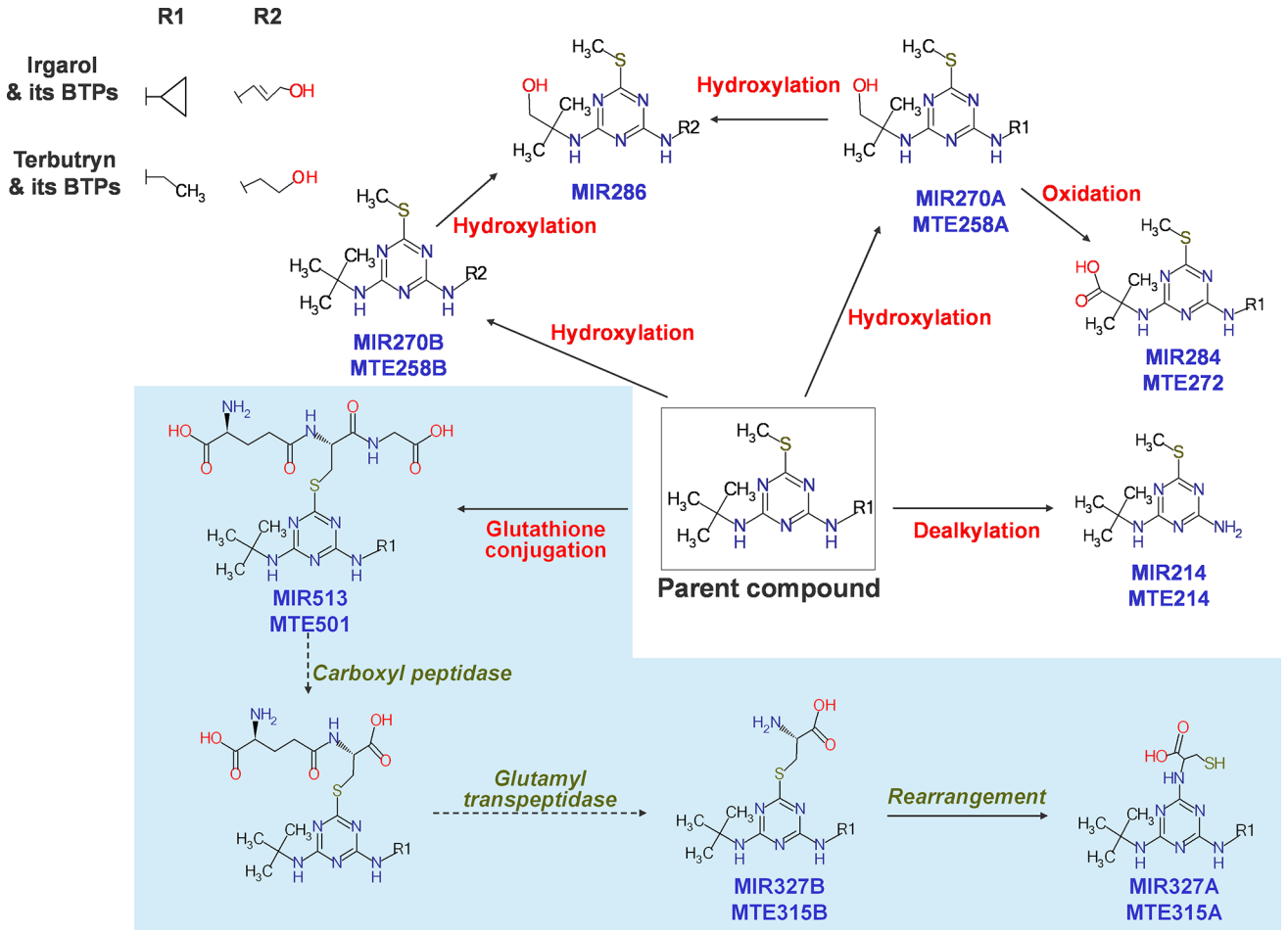

Figure 4. Proposed biotransformation pathways of irgarol and terbutryn in freshwater crustaceans. Note that R2 is the hydroxylated moiety of R1. The sky blue shaded area indicates a pathway including glutathione conjugation followed by subsequent reactions to form cysteine conjugates, reported for the first time in the test organisms.

fungus[49] and detected in surface waters.[16] The two peaks observed for the mass 270.1383 (Figure 2) were suspected oxidation products (i.e., MIR270A and B) with introduction of a hydroxyl function into the molecule at two possible sites (Figure 4). The MS/MS spectrum of MIR270A has two diagnostic fragments, m/z 73.0641 and 198.0811 (Figure 3), which give conclusive evidence for the location of the hydroxyl group on the isobutyl moiety. An almost identical MS/MS fragmentation pattern to that of MIR270B (Figure S1e (Supporting Information)) was reported in a previous study[16] for a photodegradation product of irgarol featuring an unsaturated propyl alcohol. For MIR284, the major fragment m/z 238.1123 resulted from the loss of the HCOOH moiety (characteristic loss of carboxylic acid products), while another fragment, m/z 198.0807, provided strong evidence that the carboxylic acid occurs at the isobutyl group (Figure S1f (Supporting Information)). Using these two fragments, we propose the structure of MIR284 with an amino-isobutyric acid moiety. For MIR286, modified by two oxygens, a number of diagnostic fragments or neutral losses were detected (Figure S1g (Supporting Information)). Fragment m/z 73.0645 indicated that one oxygen is attached to the isobutyl moiety, similar to that in MIR270A, while the other fragments such as m/z 158.0495, 196.0655, and 214.0764 (also measured for MIR270B) indicate that the structure of MIR286 is a hybrid of MIR270A and MIR270B, with hydroxyl functions at both isobutyl and isopropyl groups. MIR513, MIR327A, and MIR327B were identified as a glutathione conjugate and subsequent metabolites (cysteine conjugates) through the interpretation of MS/MS fragmentation patterns. A fragment of MIR327B (Figure 3c), m/z 240.1283, implied the loss of the $C_3H_5O_2N$ moiety. In addition, fragments m/z 281.1546 and 310.1340 indicated the loss of HCOOH and NH_3, respectively. This fragmentation pattern indicates that sulfur bound directly to the backbone of irgarol is linked to the $C_3H_5O_2N$ moiety, which has both $-$COOH and $-NH_2$ branches. However, MIR327A has a fragment m/z 167.1033 with six nitrogens but no sulfur, while no NH_3 loss is observed (Figure S1h (Supporting Information)). These suggested that MIR327A might be similar to MIR327B but substituting S for N, resulting in a $C_3H_5O_2S$ moiety attached to N instead of $C_3H_5O_2N$ linked to S, as suggested in the plant metabolism of atrazine.[45] The structure of MIR513 is identified as a glutathione conjugate by two diagnostic neutral losses forming fragments m/z 240.1276 and 274.1036 (Figure 3d), which both result from cleavage at the S-CH_2 bond of the precursor. In addition, loss of $C_5H_7O_3N$ is characteristic of glutathione products.[50,51]

The fragmentation patterns of the formed metabolites of irgarol and terbutryn were almost identical due to the structural similarity, with differences according to varying substituents (Figure 4). Depropylation of irgarol and deethylation of terbutryn led to the identical molecular structures MIR214 and

dx.doi.org/10.1021/tx300457f | Chem. Res. Toxicol. 2013, 26, 313−324

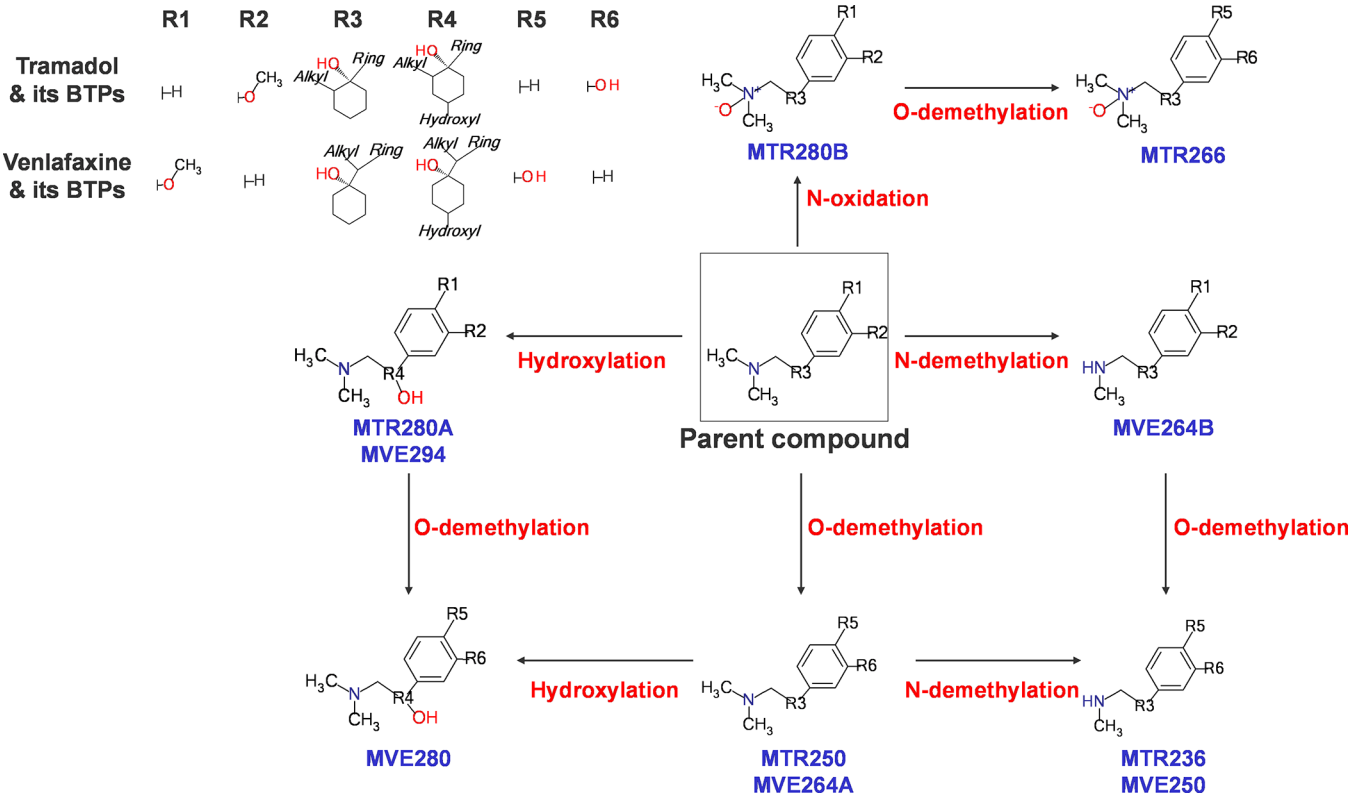

Figure 5. Proposed biotransformation pathways of tramadol and venlafaxine in freshwater crustaceans. Note that R4 is the hydroxylated moiety of R3, whereas a hydroxyl group in R5 and R6 for venlafaxine and tramadol is formed by the demethylation of R1 and R2, respectively.

MTE214, respectively. MTE214 has been considered previously as a minor photodegradation product together with a N-hydroxylation product of terbutryn.[52]

Tramadol/Venlafaxine. Tramadol and venlafaxine have an identical backbone structure, a dimethylamino- methoxyphenyl group, and showed similarities in the formation of metabolites including demethylation and oxidation products (Figure 5). Three dealkylation products of venlafaxine (i.e., MVE250, MVE264A, and MVE264B) were confirmed with reference standards. Previous studies provided MS/MS fragments of tramadol metabolites formed in horses[15] and humans[13,14] and were comparable to the analytical results for MTR266, MTR280A, and MTR280B (Figure S3e−g (Supporting Information)). The structure of the demethylation product MTR250 was determined with the diagnostic fragment *m/z* 58.0643 corresponding to C_3H_8N (Figure S3d (Supporting Information)), which implies that a methyl group is detached from oxygen not from tertiary amide, resulting in *O*-desmethyltramadol as identified elsewhere.[14] For MTR236, MVE280, and MVE294, the first ranked structures by the candidate ranking system were proposed as the most likely structures due to the lack of characteristic fragmentation information. These structures were further corroborated when considering expected but unobserved fragments for the second or third ranked structure. For example, *N,N*-didesmethyltramadol was the second best match for MTR236 but would be expected to produce NH_3 loss (characteristic of amino compound) as observed for MIR327B, MTE315B (in our study), and *N,N*-didesmethylvenlafaxine (MassBank, http://www.massbank.jp, record number EA265808), but the loss was not found in the MS/MS spectra of MTR236 (Figure S3c (Supporting Information)).

Evaluation of the Metabolite Prediction Tools and Identification Strategy. Out of the 19 oxidation products identified, the exact structures of 12 and 7 metabolites were predicted by Meteor and UM-PPS, respectively. The seven metabolites predicted by UM-PPS were all dealkylation products, whereas Meteor correctly predicted seven oxidation and five dealkylation products. Meteor prediction for conjugation products resulted mainly in glucuronidation or sulfoxidation products but not in glutathione and cysteine conjugates, which were identified in the present study. Comparing the two, we found that Meteor had a lower true negative (14 vs 19%) and false positive rate (87 vs 93%) than UM-PPS. Neither was optimal for this application because they were not developed for freshwater crustaceans. The manual prediction had the lowest true negative rate (0.5%), only two identified metabolites were unpredicted and thus are strongly recommended to complement the predictive software designed for different organisms. In addition, expert knowledge on metabolic pathways of relevant compounds found in the literature (even in different organisms) should be considered in the prediction step. Effort invested in forming a reasonable list of possible metabolites is necessary for more reliable metabolite identifications. Inappropriate predictions increase the dependence on nontarget screening and identification, which was not successful compared to the suspect screening and requires much more time and effort. Optimizations of the parameters used in SIEVE, instrument sensitivity or selectivity, and extraction procedure may have increased detection of low intensity metabolites, as well as applying a lower threshold (10^4). Altogether, the 25 metabolites we found seem to be the major products for the four target compounds and are helpful

dx.doi.org/10.1021/tx300457f | *Chem. Res. Toxicol.* 2013, 26, 313−324

to elucidate the fate of the parent compounds and biotransformation mechanisms in freshwater crustaceans.

Among a total of 25 metabolites identified in *in vivo G. pulex* samples, 15 products were also found in S9 rat liver, while 7 and 2 products were found in *G. pulex*- and *D. magna*-homogenates from *in vitro* experiments, respectively, supporting the formation of identified metabolites in test organisms. The lower number of metabolites found in *in vitro* crustacean assays indicates that the condition for enzymatic reactions was unfavorable (e.g., deactivation of enzyme activity or lack of cofactor). Nevertheless, the successful formation and detection of metabolites in the homogenate matrix verifies that the *in vitro* method is applicable for crustaceans, even though further optimization is preferable.

Metabolomics Standards Initiative (MSI) has proposed minimum reporting standards and confidence levels for metabolite identification that are classified mainly by basic spectral data (see ref 53 for the detailed definition).[53] However, Neumann and Boecker[54] pointed out that metabolite identification based on a comparison of "exact mass and isotope pattern" would be ambiguous because dozens to hundreds of compounds have a common molecular formula; thus, they emphasized the importance of structure evidence for more reliable identification. Correspondingly, we provided as structure evidence high-resolution MS/MS fragmentation patterns, which were a crucial factor in the classification of the confidence levels in our study. However, the structure elucidation with the fragmentation analysis is not always successful due to either a lack of deterministic evidence of substructure or inherent fault interpretation. Thus, all information used for structure elucidation should be open and continuously verified and shared by other experienced groups.

Biochemical Pathways, Biotransformation Reactions, and Species Differences. *Oxidation Reactions.* The hydroxylation products of irgarol and terbutryn (e.g., MIR270A, MIR270B, MIR286, MTE258A, and MTE258B) resulted from the modification at the terminal methyl group, while oxidations of tramadol and venlafaxine (MTR280A, MTR280B, and MVE294) occurred at the amine or cyclic C−H bond (Figures 4 and 5). These modified sites are all on the outer sphere of molecules where active enzymes can easily attack. This observation emphasizes the importance of accessibility of a substrate to the enzyme, favoring the least hindered bond.[55]

The formations of hydroxylation products of anthropogenic compounds in crustaceans were reported in several studies involving P450 activity.[4,42,56] In *Daphnia pulex*, CYP2D6, CYP2B6, CYP2C19, and CYP3A4 were identified, which are known to be involved in oxidative dealkylation reactions.[57,58] In case of tramadol and venlafaxine metabolism in humans, CYP2D6 was reported as the primary enzyme for O-demethylation products, whereas CYP2B6 and CYP3A4 were responsible for N-demethylation products.[59,60]

N-Dealkylation can be explained by two possible mechanisms: (1) hydroxylation of a C−H bond on the carbon adjacent to the heteroatom (H-atom transfer, HAT) and (2) a one-electron oxidation of the heteroatom itself (single-electron transfer, SET).[61] Interestingly, one study[62] observed the opening of the cyclopropyl ring adjacent to nitrogen during oxidation (also observed in the formation of MIR270B and MTE258B), strongly supporting the SET mechanism. However, O-dealkylation is a consequence of C−H bond hydroxylation (HAT mechanism).[61] In our study, O- and N-dealkylation with possibly different mechanisms were observed for venlafaxine, whereas only enzymatic O-dealkylation was found for tramadol.

Conjugation Reactions. Previous studies identified several conjugation products in aquatic crustaceans: sulfate and/or glucose conjugates of pyrene in *D. magna* and freshwater shrimp[4,63] and sulfate conjugates of aldicarb, carbaryl, and dichlorophenols in *G. pulex*.[56] Even though the activity of glutathione *S*-transferases was recommended as a biomarker for toxicity screening due to its fair sensitivity,[64,65] no GSH conjugates have been recognized in test organisms yet. The GSH conjugates MIR513 and MTE501 are expected to be formed by attack of the electrophilic methylthioether group by the reactive sulfur atom of GSH, which has been elucidated in rat metabolism upon exposures to terbutryn and prometryn.[66,67] It is known that once GSH conjugates are formed, they are subjected to additional metabolic reactions by peptidases and γ-glutamyltransferase, catalyzing sequential removal of glycyl and glutamyl moieties, respectively.[45,68] These enzymatic reactions lead to the formation of cysteine conjugates corresponding to MIR327B and MTE315B. In mammalian metabolism, the cysteine conjugates are further transformed through N-acetylation to mercapturic acids,[69,70] whereas nonenzyme reactions in a plant, *Sorghum*, rearranged *S*-cysteine to a *N*-cysteine conjugate,[45] corresponding to MIR327A and MTE315A.

The pairs sharing a common backbone, irgarol−terbutryn and tramadol−venlafaxine, showed similar molecular modification patterns. Conjugation metabolites were identified only for the former pair, which is more hydrophobic and has higher bioaccumulation potential than the latter. It seems that conjugation reactions are not necessarily triggered in freshwater organisms when a compound and its oxidation/reduction metabolites can be excreted easily without conjugations.

Species Differences. All metabolites formed in *D. magna* (11 metabolites) were also identified in *G. pulex* samples, but an additional 14 metabolites were only found in *G. pulex*. This may be due to the approximately five times less biomass and correspondingly fewer enzymes present in *D. magna* used for the extract, resulting in metabolites occurring below the LOD or evaluation threshold (10^4). However, *G. pulex* may be more active in response to xenobiotic exposures due to the difference in habitats and food sources, as well as easier induction of the detoxification enzymes upon exposure in individuals collected in the wild (i.e., *G. pulex*) compared with pure culture organisms (i.e., *D. magna*).

Information on the metabolites of irgarol and terbutryn in different species is almost unavailable (only one study for terbutryn in rats),[66] whereas a number of metabolites of tramadol and venlafaxine in mammals have been reported. In human metabolism of tramadol, N-oxidation, hydroxylation, and dealkylation are common oxidative reactions,[15] while conjugation reactions such as glucuronidation and sulfatation are reported,[13,14] these were not found in our study. In the case of venlafaxine, the major metabolic reactions in mammals include hydroxylation, demethylation, and conjugations with glucuronide or sulfate, but the metabolic pathways varied according to species.[71] In the present study, *N*-desmethylvenlafaxine (MVE264B) showed the highest intensity in *G. pulex*, whereas no metabolite of venlafaxine was identified in *D. magna*.

Future Research Needs. In the present study, we determined that oxidation reactions such as hydroxylation and demethylation as well as glutathione conjugation take place at various sites of selected compounds in freshwater crustaceans. Particularly, a pathway initiated with glutathione conjugation leading to cysteine conjugates of triazine compounds were observed for the first time in the test organisms. In addition, we confirmed the similarity in enzymatic reactions and the modified sites between different species and chemical structures. However, the outcomes and interpretations are limited to a small number of compounds. To draw more general conclusions on the relationship between the structure of xenobiotics and the metabolic pathways, many more chemical structures with a variety of functional groups need to be studied. This would simultaneously improve the prediction of metabolites, a crucial step for the time-consuming confident identification as shown in the present study. In addition, quantitative data on the formation of the metabolites are needed to explore to what extent biotransformation modifies bioaccumulation, body burden, and finally the toxicity of xenobiotics.

■ ASSOCIATED CONTENT

Supporting Information

Details on chemicals and solutions, maintenance and culture of test organisms, in vitro and in vivo experiments, LC-HRMS/MS analysis, structure candidate ranking system, software tools, and extracted ion chromatograms of parents and their metabolites. This material is available free of charge via the Internet at http://pubs.acs.org.

■ AUTHOR INFORMATION

Corresponding Author

*E-mail: Juliane.Hollender@eawag.ch.

Funding

This study was supported by funding from the Swiss National Science foundation (Grant No. 315230-141190).

Notes

The authors declare no competing financial interest.

■ ACKNOWLEDGMENTS

We thank Heinz Singer and Matthias Ruff for analytical support, Kathrin Fenner, Damian Helbling, and Hans-Peter Kohler for discussion on transformation products, Roman Ashauer and Anita Hintermeister for collection and maintenance of Gammarus, Emma Schymanski, Andreas Kretschmann, and Jennifer Schollee for structure generation (ES) and comments on the manuscript, and Michael Stravs for the MassBank database search.

■ ABBREVIATIONS

APW, artificial pond water; PP, phosphate; UM-PPS, University of Minnesota Pathway Prediction System; ESI, electrospray ionization; DDF, data-dependent MS/MS fragmentation

■ REFERENCES

(1) Van Leeuwen, C. J., and Vermeire, T. G. (2007) *Risk Assessment of Chemicals: An Introduction*, 2nd. ed., Springer: Dordrecht, The Netherlands.

(2) Howard, P. H., and Muir, D. C. G. (2011) Identifying new persistent and bioaccumulative organics among chemicals in commerce II: pharmaceuticals. *Environ. Sci. Technol. 45*, 6938−6946.

(3) Akkanen, J., and Kukkonen, J. V. K. (2003) Biotransformation and bioconcentration of pyrene in *Daphnia magna*. *Aquat. Toxicol. 64*, 53−61.

(4) Ikenaka, Y., Eun, H., Ishizaka, M., and Miyabara, Y. (2006) Metabolism of pyrene by aquatic crustacean, *Daphnia magna*. *Aquat. Toxicol. 80*, 158−165.

(5) Richter, S., and Nagel, R. (2007) Bioconcentration, biomagnification and metabolism of 14C-terbutryn and 14C-benzo[a]pyrene in *Gammarus fossarum* and *Asellus aquaticus*. *Chemosphere 66*, 603−610.

(6) Baldwin, W. S., and Leblanc, G. A. (1994) In-vivo biotransformation of testosterone by phase-I and phase-II detoxication enzymes and their modulation by 20-hydroxyecdysone in *Daphnia magna*. *Aquat. Toxicol. 29*, 103−117.

(7) McCarty, L. S., and Mackay, D. (1993) Enhancing ecotoxicological modeling and assessment. *Environ. Sci. Technol. 27*, 1719−1728.

(8) Escher, B. I., and Hermens, J. L. M. (2004) Internal exposure: Linking bioavailability to effects. *Environ. Sci. Technol. 38*, 455A−462A.

(9) Katagi, T., and Whitacre, D. M. (2010) Bioconcentration, bioaccumulation, and metabolism of pesticides in aqutic organisms. *Rev. Environ. Contam. Toxicol. 204*, 1−132.

(10) Ankley, G. T., and Collyard, S. A. (1995) Influence of piperonyl butoxide on the toxicity of organophosphate insecticides to three species of freshwater benthic invertebrates. *Comp. Biochem. Physiol., Part C: Pharmacol. Toxicol. Endocrinol. 110*, 149−155.

(11) La Farre, M., Ferrer, I., Ginebreda, A., Figueras, M., Olivella, L., Tirapu, L., Vilanova, M., and Barcelo, D. (2001) Determination of drugs in surface water and wastewater samples by liquid chromatography-mass spectrometry: methods and preliminary results including toxicity studies with *Vibrio fischeri*. *J. Chromatogr., A 938*, 187−197.

(12) Hollender, J., Singer, H., and Mcardell, C. S. (2008) Polar organic micropollutants in the water cycle. *NATO Sci. Peace Secur.*, 103−116.

(13) Wu, W. N., McKown, L. A., and Liao, S. (2002) Metabolism of the analgesic drug ULTRAM (R) (tramadol hydrochloride) in humans: API-MS and MS/MS characterization of metabolites. *Xenobiotica 32*, 411−425.

(14) Hakala, K. S., Kostiainen, R., and Ketola, R. A. (2006) Feasibility of different mass spectrometric techniques and programs for automated metabolite profiling of tramadol in human urine. *Rapid Commun. Mass Spectrom. 20*, 2081−2090.

(15) De Leo, M., Giorgi, M., Saccomanni, G., Manera, C., and Braca, A. (2009) Evaluation of tramadol and its main metabolites in horse plasma by high-performance liquid chromatography/fluorescence and liquid chromatography/electrospray ionization tandem mass spectrometry techniques. *Rapid Commun. Mass Spectrom. 23*, 228−236.

(16) Lam, K. H., Lei, N. Y., Tsang, V. W. H., Cai, Z., Leung, K. M. Y., and Lam, M. H. W. (2009) A mechanistic study on the photodegradation of Irgarol-1051 in natural seawater. *Mar. Pollut. Bull. 58*, 272−279.

(17) Okamura, H., Aoyama, I., Liu, D., Maguire, R. J., Pacepavicius, G. J., and Lau, Y. L. (2000) Fate and ecotoxicity of the new antifouling compound Irgarol 1051 in the aquatic environment. *Water Res. 34*, 3523−3530.

(18) Sinclair, C. J., and Boxall, A. B. A. (2003) Assessing the ecotoxicity of pesticide transformation products. *Environ. Sci. Technol. 37*, 4617−4625.

(19) Boxall, A. B. A., Sinclair, C. J., Fenner, K., Kolpin, D., and Maund, S. J. (2004) When synthetic chemicals degrade in the environment. *Environ. Sci. Technol. 38*, 368A−375A.

(20) Balmer, M. E., Poiger, T., Droz, C., Romanin, K., Bergqvist, P. A., Müller, M. D., and Buser, H. R. (2004) Occurrence of Methyl Triclosan, a Transformation Product of the Bactericide Triclosan, in Fish from Various Lakes in Switzerland. *Environ. Sci. Technol. 38*, 390−395.

(21) LeBlanc, A., and Sleno, L. (2011) Atrazine metabolite screening in human microsomes: detection of novel reactive metabolites and glutathione adducts by LC-MS. *Chem. Res. Toxicol. 24*, 329−339.
(22) Barbara, J. E., and Castro-Perez, J. M. (2011) High-resolution chromatography/time-of-flight MS(E) with in silico data mining is an information-rich approach to reactive metabolite screening. *Rapid Commun. Mass Spectrom. 25*, 3029−3040.
(23) Krauss, M., Singer, H., and Hollender, J. (2010) LC-high resolution MS in environmental analysis: from target screening to the identification of unknowns. *Anal. Bioanal. Chem. 397*, 943−951.
(24) Kern, S., Fenner, K., Singer, H. P., Schwarzenbach, R. P., and Hollender, J. (2009) Identification of transformation products of organic contaminants in natural waters by computer-aided prediction and high-resolution mass spectrometry. *Environ. Sci. Technol. 43*, 7039−7046.
(25) Helbling, D. E., Hollender, J., Kohler, H. P. E., Singer, H., and Fenner, K. (2010) High-throughput identification of microbial transformation products of organic micropollutants. *Environ. Sci. Technol. 44*, 6621−6627.
(26) Wittmer, I. K., Bader, H. P., Scheidegger, R., Singer, H., Luck, A., Hanke, I., Carlsson, C., and Stamm, C. (2010) Significance of urban and agricultural land use for biocide and pesticide dynamics in surface waters. *Water Res. 44*, 2850−2862.
(27) Kern, S., Baumgartner, R., Helbling, D. E., Hollender, J., Singer, H., Loos, M. J., Schwarzenbach, R. P., and Fenner, K. (2010) A tiered procedure for assessing the formation of biotransformation products of pharmaceuticals and biocides during activated sludge treatment. *J. Environ. Monit. 12*, 2100−2111.
(28) Ashauer, R., Boxall, A., and Brown, C. (2006) Uptake and elimination of chlorpyrifos and pentachlorophenol into the freshwater amphipod *Gammarus pulex*. *Arch. Environ. Contam. Toxicol. 51*, 542−548.
(29) Ashauer, R., Hintermeister, A., Caravatti, I., Kretschmann, A., and Escher, B. I. (2010) Toxicokinetic and toxicodynamic modeling explains carry-over toxicity from exposure to diazinon by slow organism recovery. *Environ. Sci. Technol. 44*, 3963−3971.
(30) Kretschmann, A., Ashauer, R., Hitzfeld, K., Spaak, P., Hollender, J., and Escher, B. I. (2011) Mechanistic toxicodynamic model for receptor-mediated toxicity of diazoxon, the active metabolite of diazinon, in *Daphnia magna*. *Environ. Sci. Technol. 45*, 4980−4987.
(31) Naylor, C., Maltby, L., and Calow, P. (1989) Scope for growth in *Gammarus pulex*, a fresh-water benthic detritivore. *Hydrobiologia 188*, 517−523.
(32) Organisation for Economic Co-operation and Development and OECD iLibrary (2004) Test No. 202: *Daphnia* sp. Acute Immobilisation Test, in *OECD Guidelines for the Testing of Chemicals, Section 2: Effects on Biotic Systems*, p 1 online resource, OECD Publishing, Paris, France.
(33) Xuereb, B., Noury, P., Felten, V., Garric, J., and Geffard, O. (2007) Cholinesterase activity in Gammarus pulex (Crustacea Amphipoda): Characterization and effects of chlorpyrifos. *Toxicology 236*, 178−189.
(34) Barata, C., Solayan, A., and Porte, C. (2004) Role of B-esterases in assessing toxicity of organophosphorus (chlorpyrifos, malathion) and carbamate (carbofuran) pesticides to *Daphnia magna*. *Aquat. Toxicol. 66*, 125−139.
(35) Ellis, L. B. M., Gao, J., Fenner, K., and Wackett, L. P. (2008) The University of Minnesota pathway prediction system: predicting metabolic logic. *Nucleic Acids Res. 36*, W427−W432.
(36) Testa, B., Balmat, A. L., Long, A., and Judson, P. (2005) Predicting drug metabolism: An evaluation of the expert system METEOR. *Chem. Biodiversity 2*, 872−885.
(37) Kind, T., and Fiehn, O. (2010) Advances in structure elucidation of small molecules using mass spectrometry. *Bioanal. Rev. 2*, 23−60.
(38) Singer, H., Jaus, S., Hanke, I., Luck, A., Hollender, J., and Alder, A. C. (2010) Determination of biocides and pesticides by on-line solid phase extraction coupled with mass spectrometry and their behaviour in wastewater and surface water. *Environ. Pollut. 158*, 3054−3064.
(39) Schymanski, E. L., Gallampois, C. M. J., Krauss, M., Meringer, M., Neumann, S., Schulze, T., Wolf, S., and Brack, W. (2012) Consensus structure elucidation combining GC/EI-MS, structure generation, and calculated properties. *Anal. Chem. 84*, 3287−3295.
(40) Benecke, C., Gruner, T., Kerber, A., Laue, R., and Wieland, T. (1997) MOLecular structure GENeration with MOLGEN, new features and future developments. *Fresenius' J. Anal. Chem. 359*, 23−32.
(41) Ashauer, R., Hintermeister, A., O'Connor, I., Elumelu, M., Hollender, J., and Escher, B. I. (2012) Significance of xenobiotic metabolism for bioaccumulation kinetics of organic chemicals in *Gammarus pulex*. *Environ. Sci. Technol. 46*, 3498−3508.
(42) Kretschmann, A., Ashauer, R., Preuss, T. G., Spaak, P., Escher, B. I., and Hollender, J. (2011) Toxicokinetic model describing bioconcentration and biotransformation of diazinon in *Daphnia magna*. *Environ. Sci. Technol. 45*, 4995−5002.
(43) Hendriks, A. J., van der Linde, A., Cornelissen, G., and Sijm, D. T. H. M. (2001) The power of size. 1. Rate constants and equilibrium ratios for accumulation of organic substances related to octanol-water partition ratio and species weight. *Environ. Toxicol. Chem. 20*, 1399−1420.
(44) Geyer, H. J., Scheunert, I., Bruggemann, R., Steinberg, C., Korte, F., and Kettrup, A. (1991) QSAR for organic-chemical bioconcentration in daphnia, algae, and mussels. *Sci. Total Environ. 109*, 387−394.
(45) Lamoureux, G. L., Stafford, L. E., Shimabukuro, R. H., and Zaylskie, R. G. (1973) Atrazine metabolism in sorghum: catabolism of the glutathione conjugate of atrazine. *J. Agric. Food Chem. 21*, 1020−1030.
(46) Anders, M. W. (2008) Chemical toxicology of reactive intermediates formed by the glutathione-dependent bioactivation of halogen-containing compounds. *Chem. Res. Toxicol. 21*, 145−159.
(47) von der Ohe, P. C., Kuhne, R., Ebert, R. U., Altenburger, R., Liess, M., and Schuurmann, G. (2005) Structural alerts: A new classification model to discriminate excess toxicity from narcotic effect levels of organic compounds in the acute daphnid assay. *Chem. Res. Toxicol. 18*, 536−555.
(48) Kazius, J., McGuire, R., and Bursi, R. (2005) Derivation and validation of toxicophores for mutagenicity prediction. *J. Med. Chem. 48*, 312−320.
(49) Liu, D., Maguire, R. J., Lau, Y. L., Pacepavicius, G. J., Okamura, H., and Aoyama, I. (1997) Transformation of the new antifouling compound Irgarol 1051 by Phanerochaete chrysosporium. *Water Res. 31*, 2363−2369.
(50) Ma, L., Wen, B., Ruan, Q., and Zhu, M. S. (2008) Rapid screening of glutathione-trapped reactive metabolites by linear ion trap mass spectrometry with isotope pattern-dependent scanning and postacquisition data mining. *Chem. Res. Toxicol. 21*, 1477−1483.
(51) Murphy, C. M., Fenselau, C., and Gutierrez, P. L. (1992) Fragmentation characteristic of glutathione conjugates activated by high-energy collisions. *J. Am. Soc. Mass Spectrom. 3*, 815−822.
(52) Ibanez, M., Sancho, J. V., Pozo, O. J., and Hernandez, F. (2004) Use of quadrupole time-of-flight mass spectrometry in environmental analysis: Elucidation of transformation products of triazine herbicides in water after UV exposure. *Anal. Chem. 76*, 1328−1335.
(53) Griffin, J. L., Nicholls, A. W., Daykin, C. A., Heald, S., Keun, H. C., Schuppe-Koistinen, I., Griffiths, J. R., Cheng, L. L., Rocca-Serra, P., Rubtsov, D. V., and Robertson, D. (2007) Standard reporting requirements for biological samples in metabolomics experiments: mammalian/in vivo experiments. *Metabolomics 3*, 179−188.
(54) Neumann, S., and Bocker, S. (2010) Computational mass spectrometry for metabolomics: Identification of metabolites and small molecules. *Anal. Bioanal. Chem. 398*, 2779−2788.
(55) Goldsmith, C. R., Jonas, R. T., and Stack, T. D. P. (2002) C-H bond activation by a ferric methoxide complex: Modeling the rate-determining step in the mechanism of lipoxygenase. *J. Am. Chem. Soc. 124*, 83−96.
(56) Ashauer, R., Hintermeister, A., O'Connor, I., Elumelu, M., Hollender, J., and Escher, B. I. (2012) Significance of xenobiotic metabolism for bioaccumulation kinetics of organic chemicals in *Gammarus pulex*. *Environ. Sci. Technol. 46*, 3498−3508.

(57) Nichols, A. I., Lobello, K., Guico-Pabia, C. J., Paul, J., and Preskorn, S. H. (2009) Venlafaxine metabolism as a marker of cytochrome P450 enzyme 2D6metabolizer status. *J. Clin. Psychopharm. 29*, 383−386.
(58) Meyer, M. R., Peters, F. T., and Maurer, H. H. (2009) Stereoselective differences in the cytochrome P450-dependent dealkylation and demethylenation of N-methyl-benzodioxolyl-butanamine (MBDB, Eden) enantiomers. *Biochem. Pharmacol. 77*, 1725−1734.
(59) Subrahmanyam, V., Renwick, A. B., Walters, D. G., Young, P. J., Price, R. J., Tonelli, A. P., and Lake, B. G. (2001) Identification of cytochrome P-450 isoforms responsible for cis-tramadol metabolism in human liver microsomes. *Drug Metab. Dispos. 29*, 1146−1155.
(60) Shams, M. E. E., Arneth, B., Hiemke, C., Dragicevic, A., Muller, M. J., Kaiser, R., Lackner, K., and Hartter, S. (2006) CYP2D6 polymorphism and clinical effect of the antidepressant venlafaxine. *J. Clin. Pharm. Ther. 31*, 493−502.
(61) Meunier, B., de Visser, S. P., and Shaik, S. (2004) Mechanism of oxidation reactions catalyzed by cytochrome P450 enzymes. *Chem. Rev. 104*, 3947−3980.
(62) Shaffer, C. L., Harriman, S., Koen, Y. M., and Hanzlik, R. P. (2002) Formation of cyclopropanone during cytochrome P450-catalyzed N-dealkylation of a cyclopropylamine. *J. Am. Chem. Soc. 124*, 8268−8274.
(63) Ikenaka, Y., Ishizaka, M., Eun, H., and Miyabara, Y. (2007) Glucose-sulfate conjugates as a new phase II metabolite formed by aquatic crustaceans. *Biochem. Biophys. Res. Commun. 360*, 490−495.
(64) Domingues, I., Agra, A. R., Monaghan, K., Soares, A. M. V. M, and Nogueira, A. J. A. (2010) Cholinesterase and glutathione-S-transferase activities in freshwater invertebrates as biomarkers to assess pesticide contamination. *Environ. Toxicol. Chem. 29*, 5−18.
(65) Barata, C., Damasio, J., Lopez, M. A., Kuster, M., de Alda, M. L., Barcelo, D., Riva, M. C., and Raldua, D. (2007) Combined use of biomarkers and in situ bioassays in *Daphnia magna* to monitor environmental hazards of pesticides in the field. *Environ. Toxicol. Chem. 26*, 370−379.
(66) Huwe, J. K., Feil, V. J., Bakke, J. E., and Mulford, D. J. (1991) Studies on the displacement of methylthio groups by glutathione. *Xenobiotica 21*, 179−191.
(67) Maynard, M. S., Brumback, D., Itterly, W., Capps, T., and Rose, R. (1999) Metabolism of [C-14]prometryn in rats. *J. Agric. Food Chem. 47*, 3858−3865.
(68) Dekant, W., and Vamvakas, S. (1993) Glutathione-dependent bioactivation of xenobiotics. *Xenobiotica 23*, 873−887.
(69) Hinchman, C. A., and Ballatori, N. (1994) Glutathione conjugation and conversion to mercapturic acids can occur as an intrahepatic process. *J. Toxicol. Environ. Health 41*, 387−409.
(70) Thompson, C. D., Gulden, P. H., and Macdonald, T. L. (1997) Identification of modified atropaldehyde mercapturic acids in rat and human urine after felbamate administration. *Chem. Res. Toxicol. 10*, 457−462.
(71) Howell, S. R., Husbands, G. E. M., Scatina, J. A., and Sisenwine, S. F. (1993) Metabolic disposition of C-14 venlafaxine in mouse, rat, dog, rhesus-monkey and man. *Xenobiotica 23*, 349−359.